Spatiotemporal Analysis and Multifactor Driving Mechanisms of Urban Blue Space in Beijing Using Remote Sensing

Ya Chen , Weina Zhen , Yu Li , Ninghui Zhang , Yishao Shi , Donghui Shi *

Posted Date: 15 August 2023

doi: 10.20944/preprints202308.1061.v1

Keywords: urban blue space; spatio-temporal analysis; mechanism simulation; landscape analysis

Article

Spatiotemporal Analysis of Urban Blue Space in Beijing and Identification of Multifactor Driving Mechanisms Using Remote Sensing

Ya Chen [1], Weina Zhen [2,3], Yu Li [2,3], Ninghui Zhang [2,3], Yishao Shi [4] and Donghui Shi [2,*]

[1] School of Marxism, Beijing Forestry University, Beijing, 100083, China;
[2] Institute of Geographic Sciences and Natural Resources Research, Chinese Academy of Sciences, Beijing, 100101, China
[3] College of Resources and Environment, University of Chinese Academy of Sciences, Beijing, 100049, China
[4] College of Surveying and Geo-Informatics, Tongji University, Shanghai 200092, China;
* Correspondence: shidonghui@igsnrr.ac.cn; Tel.:+86-188-1787-9804

Abstract: With the rapid urban development in Beijing, there is a critical need to explore urban natural resources and understand the underlying mechanisms. Urban blue space (UBS) has gained increasing attention due to its potential to drive microcirculation, mitigate heat islands, and enhance residents' well-being. In this study, we used remote sensing data to extract UBS in Beijing and employed exploratory spatial data analysis (ESDA) methods to examine its spatial and temporal development over the past two decades. We adopted a mesoscopic perspective to uncover the full spectrum of landscape patterns and quantitatively simulate the mechanisms influencing the area of UBS and landscape patterns. Our findings are as follows: (1) The UBS area in Beijing exhibited fluctuating growth from 2000 to 2020. (2) Spatial clustering of UBS was stable with subtle changes. (3) The ecological conditions in Beijing improved over the last 21 years indicated by increased habitat diversity and richness, while notable landscape fragmentation posed significant challenges. (4) Technological factors emerged as the most influential mechanism for the UBS area, followed by vegetation conditions represented by the normalized difference vegetation index (NDVI) and annual average temperature (T).(5) Precipitation emerged as the most vital influencing factor for the UBS landscape, followed by residential population (POP) and economic conditions represented by gross domestic product (GDP).(6) The density of the vegetation surface, as indicated by the gap between the NDVI and enhanced vegetation index (EVI), proved more sensitive to the UBS area than to the UBS landscape.

Keywords: urban blue space; spatiotemporal analysis; mechanism simulation; landscape analysis

1. Introduction

Urban blue space (UBS) refers to spaces of surface water within urban areas, including lakes, channels, and pools [1]. UBS plays a crucial role in various aspects, such as biodiversity conservation [2], climate change mitigation [3], provision of ecosystem services[4], and public health benefits [5]. It also contributes to reducing the heat island effect and regulating the local climate [6–8]. Consequently, the management of UBS holds great importance in urban planning and development [9,10]. In addition to its functional benefits, UBS significantly enhances the aesthetics [11] and cultural value [12] of urban environments. It provides a sense of comfort and tranquility, offering respite from the pressures of modern city life [13,14]. Furthermore, UBS helps mitigate flood risks associated with the expansion of artificial surfaces, optimizes land use patterns, improves public satisfaction, and promotes residents' well-being [15–19].In Beijing, as a globally recognized metropolis renowned for its fast-paced lifestyle, serves as an exemplary case study for examining the role of UBS in urban environments.

 doi:10.20944/preprints202308.1061.v1

In terms of the content of existing studies in this field, the focus has primarily been on changes in urban blue spaces (UBS) [20] and patch connectivities [21–23]. However, UBS in metropolises serve not only as functional outdoor water bodies but also as unique urban landscapes and spaces with aesthetic and emotional significance. Therefore, it is crucial to pay more attention to the area and landscapes of UBS. Regarding the time scale, most previous research has concentrated on specific years or short-term timelines [24–28]. However, UBS changes occur over long-term and gradual processes, which cannot be adequately captured within a short-term study spanning only three to five years [29]. Additionally, UBS is subject to irregular impacts from extreme weather events such as droughts and floods, which are often overlooked when using equal time interval methods [30]. Hence, conducting long-term studies with more detailed information is essential in this field. In terms of primary data, previous research on UBS landscapes has primarily relied on traditional data sources, such as historical maps and aerial images with large spatial resolutions and limited information [31,32]. These sources only support studies at a patch scale [33,34]. However, with advancements in remote sensing technology, high-quality primary data have become more accessible. Therefore, there is a demand for studies that utilize more detailed information and focus on a smaller scale [35,36]. Considering the potential interference of fragmented and temporal water patches resulting from high-resolution data, as well as the inability of low-resolution data to capture detailed information, this study adopts remote sensing data with a resolution of 30 m × 30 m to accurately extract UBS.

The analysis of component mechanisms, including population, economics, climate, and land use [37], deserves more attention compared to single-factor studies [38] since the spatiotemporal characteristics of UBS are influenced by multiple resource factors. Understanding the interactions and contributions of these factors is crucial in comprehending UBS dynamics. Moreover, qualitative mechanisms hold greater value for policymakers and stakeholders [39–43] involved in urban management and hydrological projects compared to quantitative mechanisms [44,45]. Qualitative insights provide a deeper understanding of the underlying processes and offer more meaningful guidance for decision-making. In many existing studies, the differentiation in vegetation density has been overlooked [46]. However, vegetation density directly affects the water holding capacity and the ability of ecosystems to regulate runoff. Considering that the area of low-density vegetation in Beijing is significantly larger than that of high-density vegetation and that the availability of vegetation density data is limited, the authors have chosen NDVI, which is more sensitive to low-density vegetation surfaces, and EVI, which is more sensitive to high-density vegetation surfaces [47], as proxies to distinguish vegetation density in this study.

Compared to previous studies, this research makes several significant contributions. First, the authors have chosen a sequential 21-year period, which helps avoid information gaps that may occur in previous studies using equal interval methods. By analyzing a longer time span, a more comprehensive understanding of UBS dynamics can be achieved. Second, in terms of spatial and temporal analysis, the remote sensing data utilized in this study offer wider coverage, increased accuracy, and more detailed information compared to traditional data sources such as urban planning drawings and surveying statistics used in previous studies. This enables a more robust and nuanced investigation of urban landscapes. Finally, this research explores the heterogeneity in vegetation density within the mechanism simulation, which has often been overlooked in existing studies. By considering variations in vegetation density, the study provides insights into the impact of different vegetation types and their densities on UBS dynamics. This contributes to a more comprehensive understanding of the mechanisms driving UBS changes.

2. Materials and Methods

2.1. Study Area

The study area of this research is Beijing, which is a prominent political, economic, and cultural center in China. Beijing is situated between 115.7°E - 117.4°E longitude and 39.4°N - 41.6°N latitude [48]. It shares borders with Tianjin in the east and Hebei in the remaining directions (see Figure 1).

Preprints (www.preprints.org) | NOT PEER-REVIEWED | Posted: 15 August 2023 doi:10.20944/preprints202308.1061.v1

The city covers an area of 16,410 square kilometers and had a permanent resident population of 21.89 million as of 2021 [49]. Beijing experiences a monsoon-influenced humid continental climate. Summers in Beijing are hot, humid, and prone to rainfall, while winters are cold, dry, and characterized by clear skies. The average annual rainfall in Beijing is approximately 698.4 mm, and the average annual temperature ranges from 9°C to 19°C [50].

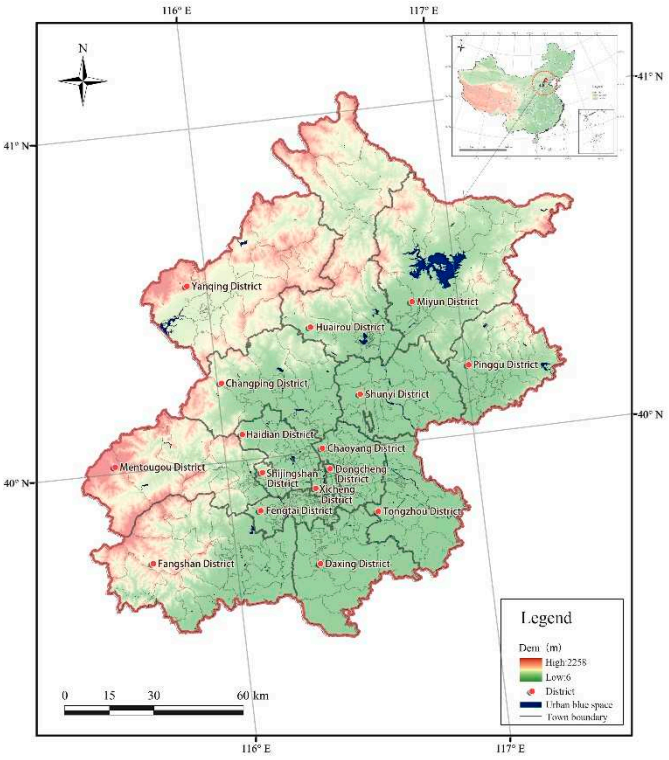

Figure 1. Study Area of Beijing.

Beijing serves as a typical case for studying urban blue space (UBS) in a metropolis. The city's UBS plays a crucial role in several aspects. First, due to the frequent intense rainfall and extreme precipitation events that occur during the summer, UBS serves as a vital component of natural reservoirs, helping to absorb and regulate excess water, thereby reducing the risk of flooding. Additionally, UBS in Beijing provides valuable mental and recreational benefits to the public. As a special urban landscape, UBS is a source of mental relaxation and entertainment for the city's residents amidst their fast-paced lives. These blue spaces create a serene and tranquil environment, offering an escape from the hustle and bustle of urban life. The presence of UBS in Beijing contributes to the overall well-being and quality of life for its inhabitants. Considering the dual functions of flood mitigation and mental well-being, studying UBS in Beijing provides valuable insights into the multifaceted role of blue spaces in metropolises.

2.2. Methodology

2.2.1. Spatial Autocorrelation Analysis and Spatial Clustering Analysis

Spatial autocorrelation detects the convergence or dispersion of observations [51,52]. Moran's I is a widely used classical spatial autocorrelation index. For a series of n variable samples, x_i is the observation at location i, and w_{ij} is the spatial weight matrix (SWM). Then, Moran's I is calculated as follows:

$$I = \frac{n\sum_{i=1}^{n}\sum_{j=1}^{n} w_{ij}(x_i - \bar{x})(x_j - \bar{x})}{\sum_{i=1}^{n}\sum_{j=1}^{n} w_{ij}\sum_{i=1}^{n}(x_i - \bar{x})^2}$$

Moran's I ranges from -1 to 1. Moran's I >0 indicates a positive spatial correlation. The closer it is to 1, the more significant the positive spatial autocorrelation. Moran's I < 0 indicates a negative

Preprints (www.preprints.org) | NOT PEER-REVIEWED | Posted: 15 August 2023 doi:10.20944/preprints202308.1061.v1

spatial correlation. The closer it is to -1, the more significant the negative spatial autocorrelation. Moran's I =0 means a random distribution [53]. The high/low clustering (Getis-Ord General G*) tool is an effective method for spatial aggregation simulation. The calculation formula is as follows:

$$G^*=\frac{\sum_{j=1}^{n} w_{ij}x_j-\bar{x}\sum_{j=1}^{n} w_{ij}}{\sqrt{\frac{\sum_{j=1}^{n} x_j^2}{n}-\frac{1}{x^2}}\sqrt{\frac{\left[n\sum_{j=1}^{n} w_{ij}^{w}-\left(\sum_{j=1}^{n} w_{ij}\right)^2\right]}{n-1}}}$$

$\bar{x}$ is the average of observations, $x_1,\ x_2,\cdots,x_n$ w_{ij} is the spatial weight of x_i and x_j, $i,j=1,2,\cdots,n$. The higher G* is, the higher the observation clustering, and vice versa. The null hypothesis of General G* assumes that the observations do not cluster spatially [54]. The p value determines whether the null hypothesis should be accepted or not. The z score reflects the dispersion of observations [55].

2.2.2. Principal Components Regression Analysis

Principal component regression analysis (PCR) is used to solve multivariate collinearity problems [56]. Principal component analysis (PCA) converts multiple indexes into several comprehensive indexes by orthogonal rotation transformation, following the premise of minimizing information loss. Generally, the results of PCA are independent variables called principal components [57]. The geometric interpretation and model of PCA are as follows (Figure 2):

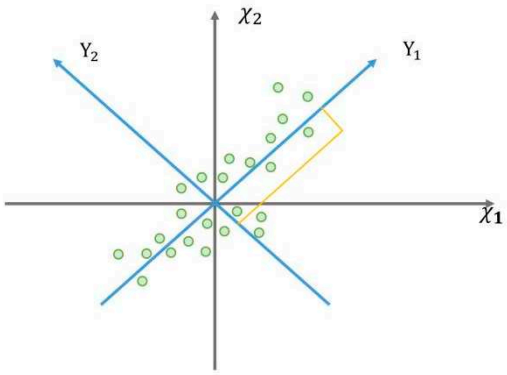

Figure 2. Illustration of principal component analysis theory.

The distribution of a series of n binary observations $(x_{11},x_{12},\cdots,x_{n1},x_{n2})$ in the coordinate space composed of X_1 and X_2 is shown in Figure 2. Along the X_1 or X_2 axis, observation points have large discretization indicated by the variance of X_1 or X_2, respectively. Axes X_1 and X_2 are rotated counterclockwise to axes Y_1 and Y_2 following formula X. The dispersion of n observation points on the Y_1 axis is the largest, indicating that variable Y_1 retains most of the information of the original data.

$$\begin{pmatrix}Y_1\\Y_2\end{pmatrix}=\begin{pmatrix}\cos\theta & \sin\theta\\-\sin\theta & \cos\theta\end{pmatrix}\begin{pmatrix}X_1\\X_2\end{pmatrix}=UX$$

2.2.3. Grey Relation Analysis

A complex system always involves various elements; the mechanism of each element is hard to simulate quantitively in practice because of the associated interactions. Grey system theory attempts to look for quantitative relationships based on the curve geometry [58-60]. Sequences are closely related when they have tight geometry curves and similar trends, and vice versa. Thus, grey correlation analysis is an effective classical quantitative measure for dynamic series. The formula is as follows:

$$r\left(x_0(k),x_i(k)\right)=\frac{\min\limits_i\min\limits_k|x_0(k)-x_i(k)|+\xi\max\limits_i\max\limits_k|x_0(k)-x_i(k)|}{|x_0(k)-x_i(k)|+\xi\max\limits_i\max\limits_k|x_0(k)-x_i(k)|}$$

Preprints (www.preprints.org) | NOT PEER-REVIEWED | Posted: 15 August 2023 doi:10.20944/preprints202308.1061.v1

$$r(x_0, x_i) = \frac{1}{n}\sum_{k=1}^{n} r(x_0(k), x_i(k))$$

where $r(x_0(k), x_i(k))$ is the grey correlation coefficient at location k, $r(x_0, x_i)$ is the data sequence from x_0 to x_i. ξ refers to the resolution coefficient. The value of ξ is inversely proportional to the difference between sequence phases. In classical statistical theory, for a set of observations with a large sample size, the probability of the sample is approximately equal to the frequency. Thus, ξ is equal to 0.5.

2.3. Data and Resources

Remote sensing images from the Google Earth Engine data catalog were used to extract influencing factors. The statistical data were retrieved from the statistical yearbook and official websites (Table 1).

Table 1. Data and resources.

Number	Name	Dataset	Spatial resolution	Temporal resolution
1	POP	Gridded Population of the World, Version 4	100 m	Yearly
2	PREP	ERA5-Land	0.1° *0.1°	Daily
3	T	Aqua/Terra MODIS MYD11A2	1000 m	Eight days
4	FVC	MODIS MCD12Q1	500 m	Yearly
5	ASP	MODIS MCD12Q1	500 m	Yearly
6	NDVI	MODIS NDVI MYD13Q1 V6	250 m	Sixteen days
7	EVI	MODIS NDVI MYD13Q1 V6	250 m	Sixteen days
8	GDP	Beijing Statistical Yearbook; Beijing Statistical Bulletin of National Economic and Social Development	–	Yearly
9	UEM	Beijing and each district's statistical yearbook	–	Yearly
10	EDUI	Beijing and each district's statistical yearbook	–	Yearly
11	STI	Beijing and each district's statistical yearbook	–	Yearly
12	UBS	JRC Monthly Water History, v1.3	30 m	Monthly

To address the spatial and temporal resolution differences between remote sensing images and statistical data, the influencing factors derived from remote sensing images were aggregated to the district level from the pixel scale. This aggregation process ensures that the data align with the resolution of the statistical data available. Furthermore, to account for the temporal variations within the remote sensing images, the data were further derived to annual averages. This averaging process provides a representative value for each influencing factor, smoothing out short-term fluctuations and capturing the overall trends over time. By aggregating and deriving the data, this study ensures compatibility and consistency between the remote sensing images and the available statistical data, enabling a comprehensive and integrated analysis of the influencing factors at the district level on an annual basis (Figure 3).

Preprints (www.preprints.org) | NOT PEER-REVIEWED | Posted: 15 August 2023 doi:10.20944/preprints202308.1061.v1

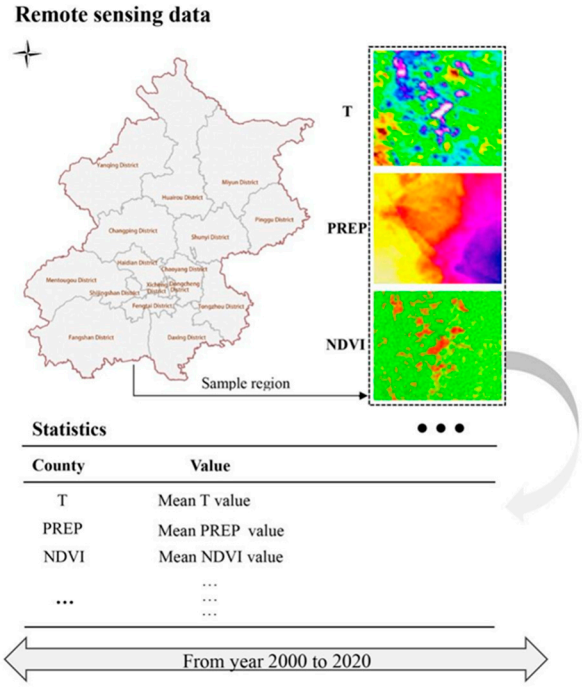

Figure 3. Multi-resoure data analysis method.

Referring to the existing research, considering the actual situation and data availability in Beijing, the authors have selected the following indicators as influencing factors for studying UBS.

Population(POP): Population is a critical factor influencing UBS scope and intensity[61,62]. Domestic water consumption and modifications to surface runoff by human activities significantly impact UBS. Therefore, population is a relevant indicator in this study.

Precipitation(PREP): Urban precipitation plays a vital role in the groundwater recharge and overall water circulation in cities . Extreme weather events associated with global climate change can generate temporary urban blue spaces, such as groundwater puddles. Hence, precipitation is commonly considered an influential indicator in UBS research [63].

Temperature(T): UBS and temperature represent a complex system interactions. UBS helps regulate the local microclimate, mitigating high temperatures and providing substantial cooling effects to the surrounding areas [64]. Higher temperature accelerates waterbody shrinking through increased evaporation. Thus, temperature is a significant factor to consider in UBS studies [65].

Fractional vegetation cover(FVC): Vegetation plays a crucial role in slowing surface runoff and enhancing water conservation capacity[66,67]. Considering the positive influence of vegetation on UBS, FVC is an essential indicator in this study.

Artificial surface proportion(ASP): The proportion of artificial surface in a city significantly affects its surface temperature, leading to either warming or cooling effects. Analyzing ASP helps in understanding urban ecological health and the impact of ASP on UBS [68].

Normalized difference vegetation index: NDVI is closely associated with the cooling effect of urban ecological spaces and precipitation[69]. It is more sensitive than the enhanced vegetation index (EVI) in regions with sparse vegetation, which are often found in metropolises such as Beijing. Thus, NDVI is a suitable indicator for UBS research in Beijing.

Enhanced vegetation index(EVI): EVI is a robust remote sensing index that reflects vegetation density and is especially effective for dense vegetation surfaces. It is closely related to urban microcirculation and blue spaces [70].

Gross domestic product(GDP): GDP measures the gross product of a country and indirectly reflects water consumption, wastewater discharge, and water-use efficiency [71,72]. Considering the implications for water management and efficiency, GDP is a relevant indicator in this study.

Preprints (www.preprints.org) | NOT PEER-REVIEWED | Posted: 15 August 2023 doi:10.20944/preprints202308.1061.v1

Urban environmental management (UEM): UEM encompasses water conservancy, public facilities, and land use planning to ensure that population growth is in alignment with access to natural resources, basic infrastructure, and shelter. UEM, including water management, precipitation collection, and hydrological services, is directly related to UBS.

Educational investment (EDUI): Education investment significantly promotes science and technology, which in turn affects production methods and water consumption efficiency. It is closely related to UBS and its sustainability.

Scientific and technical investment (STI): STI drives the application of technologies such as the Internet of Things (IoT), YunOS IoT, and big data. These technologies optimize water consumption patterns and UBS planning, making STI a relevant indicator in understanding UBS dynamics.

3. Results

3.1. Spatiotemporal Analysis of Blue Space Area

3.1.1. Development Characteristics of the UBS Area in Beijing

The UBS area in Beijing showed a slight increasing trend from 2000 to 2020, with a stable trend from 2004 to 2016. It has been clearly upward since 2016. The area of UBS in Beijing was 124.4 km² in 2000, reducing to 99.08 km² in 2004, rising slightly to 121 km² in 2016, and increasing to 183.4 km² in the last four years (Figure 4).

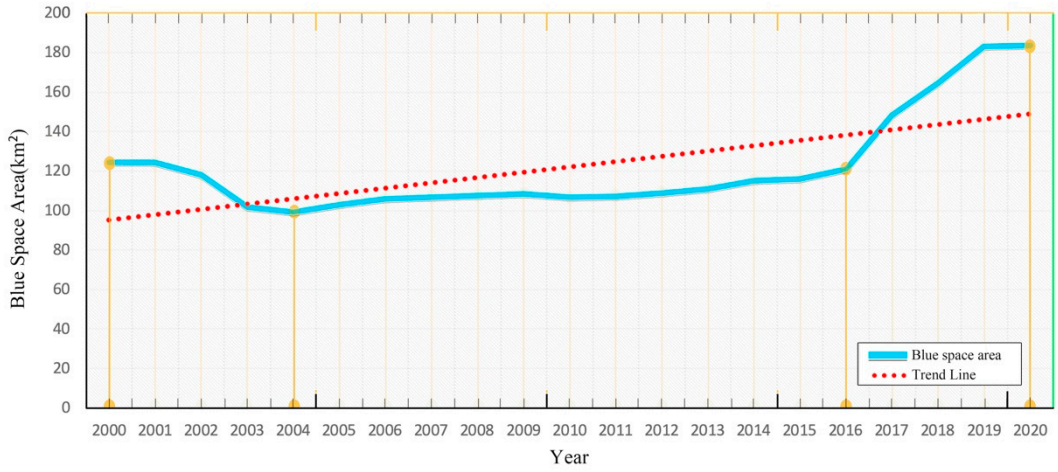

Figure 4. The area of UBS in Beijing from 2000 to 2020.

3.1.2. Spatial Autocorrelation Analysis of the UBS in Beijing

Considering a confidence level of α=0.05, Moran's I is always lower than 0.2, which means that the UBS exhibited a random distribution.

3.1.3. Spatial Clustering Pattern of the UBS in Beijing

From 2000 to 2020, the cluster analysis of "high/low" revealed that the agglomeration characteristics of UBS were relatively stable at the county level. However, the significance of clustering in Tai Shitun decreased prominently (Figure 5).

Preprints (www.preprints.org) | NOT PEER-REVIEWED | Posted: 15 August 2023 doi:10.20944/preprints202308.1061.v1

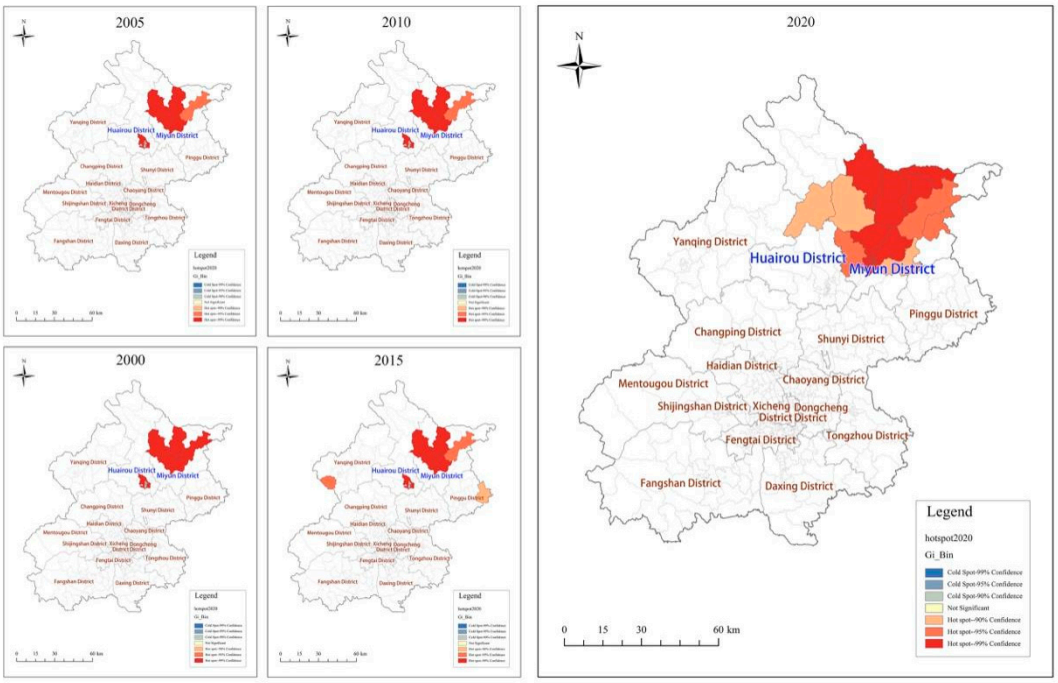

Figure 5. Spatial clustering pattern of the UBS in Beijing.

3.2. Spatiotemporal Analysis of the UBS Landscape in Beijing

3.2.1. Analysis of Landscape Indicators

Landscape pattern comprehensively reflect landscape spatial heterogeneity. Patterns reveal the spatial distribution and combination of different patches. These patches are always of various sizes, shapes, and attributes.

In this study, multiple landscape indexes were computed. Specific indicators included LPI, SPLIT, CONTAG, AI, PD, NP, LSI, SHDI, SHEI,and PAFRAC. The detailed descriptions and formulas of these indicators are presented in Table 2 [73].

Table 2. Landscape indexes.

LPI（Largest patch index）	Area percentage of maximum patch
SPLIT (Splitting index)	Dispersion among different patches at a landscape scale. The higher the value of SPLIT, the more separation between studied patch types.
CONTAG (Contagion index)	Spatial collection and decentralization. The smaller the value of CONTAG, the more sparse each patch type.
AI（Aggregation index）	Connectivity between patches of all patch types. The lower the value is, the more discrete the landscape.
PD (Patch density)	Patch density in the landscape reflects the degree and type of landscape fragmentation. Patch density represents the spatial heterogeneity of the landscape per unit area.
NP (Number of patches)	Number of all patches distributed in the landscape.

 doi:10.20944/preprints202308.1061.v1

LSI (Landscape shape index)	Indicates the change in landscape form. The higher the value, the more complex the shape.
SHDI (Shannon's diversity index)	Reflects how many different quantitative measures are in a dataset.
SHEI (Shannon's evenness index)	Describes the extent of the landscape controlled by minority patch types.
PAFRAC (Perimeter area fractal dimension)	The intensity index reflects the disturbance in landscape patterns due to human activities. The higher the value, the greater the landscape's external disturbance.

The elements with upward trends: are LPI, SPLIT, PD, NP, LSI, SHDI, SHEI, and PAFRAC (Figure 6). Their changes show that UBS landscape pattern in Beijing developed stably in the first two decades. The maximum landscape patch area is increasing. Patches are more complex and have a significant change intensity. Diversity and richness are improved. The patches are distributed more evenly. Landscape patch types have become more diverse because of human effects. As a result, the extent of separation, fragmentation, and spatial heterogeneity indexes was more remarkable and higher.

The indicators with downward trends: are AI, CONTAG (Figure 6). In the last 21 years, the landscape connectivity of UBS in Beijing has been shallow, and the downward trend was kept up with the sprawl of urban construction.

Preprints (www.preprints.org) | NOT PEER-REVIEWED | Posted: 15 August 2023 doi:10.20944/preprints202308.1061.v1

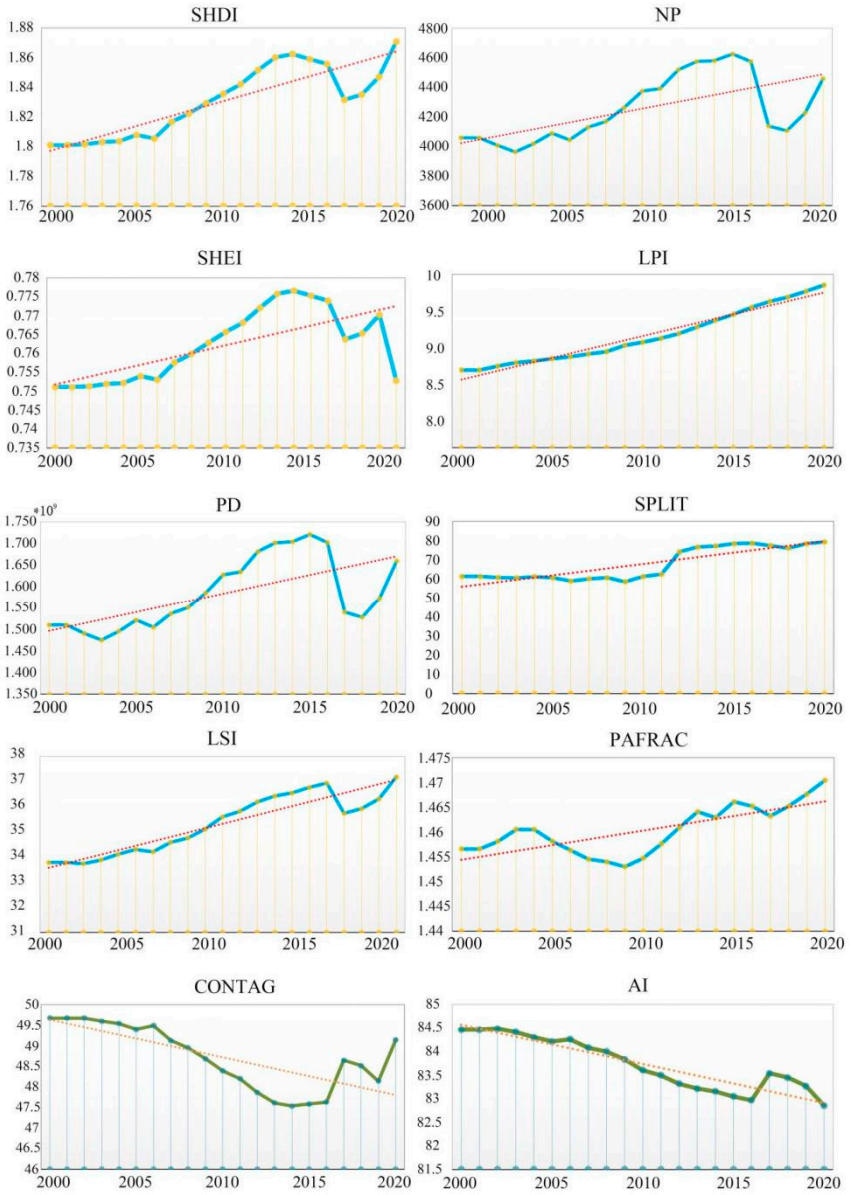

Figure 6. Landscape indexes development from 2000 to 2020.

3.2.2. Principal Component Analysis of the UBS Spatial Landscape Indices

The cumulative contribution rate of the first two principal components (Z_1 and Z_2) is 93.9% (Table 3), indicating that the first two principal components contain 93.9% of the information of the 10 original components. Thus, the landscape indexes of the UBS could be significantly extracted to the two component indicators (Formula 1, 2).

Table 3. Results of principal component analysis.

component	eigenvalue	contribution rate	cumulative contribution rate
1	8.162	81.623	81.623
2	1.228	12.280	93.903
3	0.328	3.276	97.179
4	0.222	2.224	99.403
5	0.043	0.427	99.830
6	0.014	0.140	99.970
7	0.003	0.029	99.999

Preprints (www.preprints.org) | NOT PEER-REVIEWED | Posted: 15 August 2023 doi:10.20944/preprints202308.1061.v1

8	0.000	0.001	100.000
9	0.000	0.000	100.000
10	0.000	0.000	100.000

$$Z_1=0.925NP+0.925PD+0.384LPI+0.735LSI+0.156PAFRAC-0.913CONTAG+0.456SPLIT+0.784SHDI+0.895SHEI-0.736AI \quad (1)$$

$$Z_2=0.295NP+0.295NP+0.881LPI+0.66LSI+0.946PAFRAC-0.32CONTAG+0.855SPLIT+0.587SHDI+0.273SHEI-0.659AI \quad (2)$$

Z_1 is highly positively related to NP, PD, SHEI and negatively related to CONTAG, indicating a spatial distribution structure at a landscape scale. The higher the Z_1, the greater the NP, PD, and SHEI indexes, and the smaller the CONTAG value, indicating more patches, the higher patch density, the lower agglomeration degree of various patches, and the higher patch diversity. Z_2 is positively related to PAFRAC, LPI, and SPLIT, reflecting spatial distribution structure at the patch scale. The higher the Z_2, the greater the PAFRAC, LPI, and SPLIT indexes, meaning a more complex patch shape, the more extensive patch area, and greater distance between patches.

Z_1 increased steadily from 2000 to 2014 and decreased until 2020, with a downward trend overall. The results revealed that UBS patch number, density, and diversity had increased at fourteen years and then declined in the last six years; the agglomeration weakened and then decreased. Overall the UBS in Beijing has faced severe fragmentation, which is expected to slow in recent years.

In contrast, Z_2 decreased in the first decade and increased in the second decade, trending upward. The results showed that the shape complexity, area, and distance decreased first and then increased. From the perspective of the whole period, the UBS in Beijing was disturbed from 2000 to 2020 and has been declining in the last decade.

3.3. Mechanisms Driving the Area of UBS

According to the correlation coefficients, the influencing factors rated from most to least importance are as follows: UEM>EDUI>STI>NDVI>T>GDP>POP>FVC>EVI>PREP>ASP.

The influencing factors were identified as strong factors (UEM, EDUI, STI), medium factors (NDVI, T, GDP, POP), and weak factors (FVC, EVI, PREP, ASP) according to Jenks Natural Breaks Classification.

The results showed that scientific technology factors greatly influenced the UBS area, with correlation coefficients greater than 0.7. The strongest factor is UEM, with the highest coefficient of 0.798, followed by EDUI and STI, with coefficients of 0.759 and 0.758, respectively. The coefficients of NDVI and EVI indicated that the sparse vegetation surface magnified the UBS area more than the dense vegetation surface.

3.4. Mechanisms Influencing the UBS Landscape

From the perspective of UBS landscapes, the influencing factors were rated as follows: PREP> POP> GDP>STI>T>EDUI>UEM>ASP>NDVI>EVI>FVC (Table 4). According to the results of the Jenks Natural Breaks Classification, the strong factors influencing the UBS landscape are PREP, POP, GDP, STI, and T, the medium factors are EDUI, UEM, and ASP, and the weak factors are NDVI, EVI, and FVC. Thus, it is reasonable to conclude that precipitation and human activities influence the UBS landscape more than vegetation factors.

Table 4. Correlation analysis of UBS area and landscapes.

Influencing Factors	Correlation Coefficients of UBS Area	Correlation Coefficients of UBS Landscapes
UEM	0.798	0.664
EDUI	0.759	0.665
STI	0.758	0.686
NDVI	0.697	0.617

Preprints (www.preprints.org) | NOT PEER-REVIEWED | Posted: 15 August 2023 doi:10.20944/preprints202308.1061.v1

T	0.692	0.685
GDP	0.689	0.691
POP	0.68	0.692
FVC	0.659	0.493
EVI	0.658	0.585
PREP	0.62	0.732
ASP	0.5	0.656

4. Discussion

The UBS area initially decreased from 2000 to 2004 due to significant water consumption resulting from population growth and industrial activities, leading to water shortages [74]. However, a series of measures aimed at improving water resources and protecting urban water bodies subsequently led to a steady expansion of the UBS area. The implementation of the South–North Water Diversion Project, which began in late 2014, significantly contributed to the increase in UBS area [75]. The year 2016 stands out in particular with a sharp increase in UBS area, which can be explained by the significantly greater annual precipitation since 2015 [76] and the changes in water availability and management practices after the South–North Water Diversion Project (Figure 7). These findings align with previous research [77].

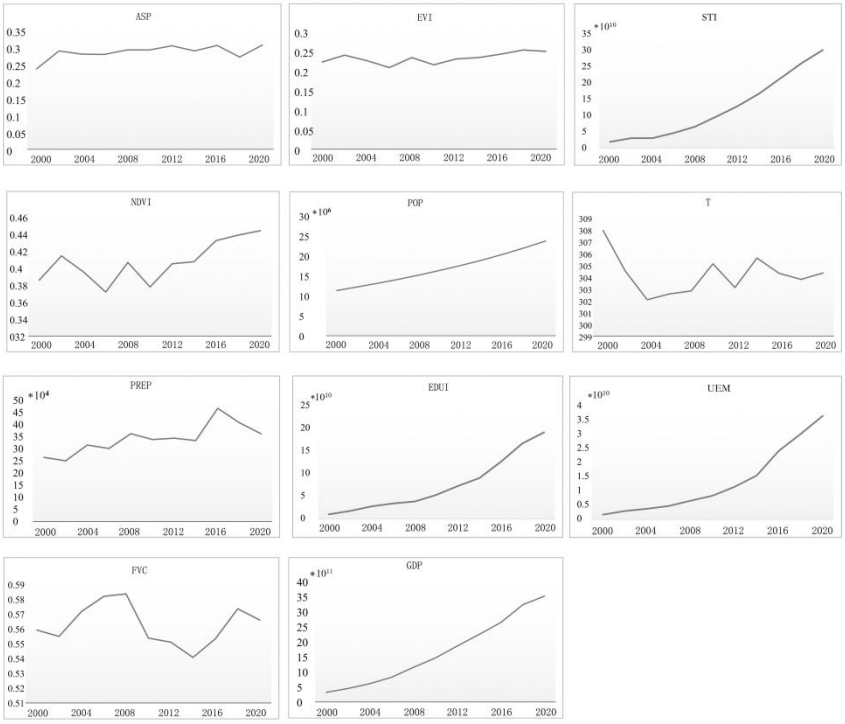

Figure 7. Development of influencing factors.

The landscape pattern of UBS in Beijing showed stability with increasing diversity, richness, and evenness indexes from 2000 to 2020, indicating the generation of more water bodies with diverse properties and purposes. However, the dispersion and spatial heterogeneity indexes were poor, indicating severe fragmentation potentially caused by urban expansion and the erosion of ecological spaces [78]. Water pollution policies implemented since 2015 have helped improve water microcirculation, leading to a reversal of negative trends in 2017, with decreasing density and diversity indexes and increasing connectivity and aggregation indexes.

The spatial distribution of UBS in Beijing appeared random, potentially influenced by artificial water bodies created in heat island-reducing projects over the past two decades [79]. Stable UBS clustering patterns were observed, with unique spots identified, such a shrinking clustering in

Taishitun County, extinct clustering in Huairou District, and expanded clustering in Miyun District. Regulation policies, such as vegetable cultivation, reservoir water network development, and reclaimed water usage, are likely related to stable development and clustered expansion. Conversely, decreasing and extinct clusterings could be attributed to disturbances from industrial and agricultural consumption, river channel changes, and artificial water bodies [80].

Among the 11 influencing factors, scientific technology factors have a strong impact on the UBS area, while precipitation and human activities strongly influence UBS landscapes. Scientific technologies enhance production efficiency and water utilization efficiency, reducing water consumption and expanding the UBS area. Precipitation replenishes water storage in urban water bodies and promotes vegetation growth, directly affecting the landscape pattern of the UBS. Human activities, including land use changes and surface modifications, have a direct and significant impact on UBS landscapes. Medium influencing factors, such as sparse vegetation, temperature, economy, and population, have a moderate influence on UBS area and landscapes. Weak factors are associated with land use patterns, particularly in dense vegetation areas, reflecting the limited correlation in these regions [81]. The weak influencing factors in UBS landscapes are closely related to vegetation.

5. Conclusions

The authors of this study utilized remote sensing techniques to extract urban blue space (UBS) in Beijing. They conducted a comprehensive analysis of the spatial and temporal development of UBS in the past two decades using ESDA methods. From an ecological perspective, they examined the full spectrum of landscape patterns and quantitatively simulated the mechanisms of UBS area and landscape changes. The findings revealed that the UBS area in Beijing experienced a decline from 2000 to 2004, followed by a steady increase over the next decade and a significant jump since 2016. The spatial clustering of UBS displayed overall stability with subtle changes. The landscape analysis indicated improvements in ecological circumstances, including increasing habitat diversity and richness, although challenges related to landscape fragmentation were observed. These results underscored the value of ecological projects initiated by the government and public organizations [82].

In terms of mechanisms influencing UBS area, all factors except for artificial surface proportion (ASP) exhibited significant influence, with correlation coefficients greater than 0.6. Scientific technologies emerged as the most influential driver, followed by natural climate factors. Human activities, such as economy and population, showed a weaker influence, while artificial surfaces had the weakest impact. Regarding UBS landscape patterns, natural climate and human activities were identified as the strongest influencing factors, whereas factors related to vegetation showed a weaker influence.

The normalized difference vegetation index (NDVI) and enhanced vegetation index (EVI), which indicate the conditions of dense and sparse vegetation regions, respectively, exhibited distinct influences on UBS area and similar impacts on UBS landscape patterns.

This study successfully uncovered the spatiotemporal characteristics of the UBS area and landscapes in Beijing from 2000 to 2020 and elucidated the multifactorial mechanisms driving these changes. However, the analysis resolution was limited to counties due to the availability of policy number and statistics data, rather than at the pixel level. Further research is needed to explore UBS at a finer scale.

Additionally, while the study analyzed 11 influencing factors, it is acknowledged that there may be other factors that should have been explored, such as the number and effectiveness of policies. Furthermore, due to data limitations, the study focused on a 21-year period, and longer-term research is warranted in the future.

Author Contributions: D.S. Conceptualization, D.S. W.Z. and Y.C.; Methodology, Y.C., D.S. and W.Z.; Software, Y.L. and N.Z.; Validation, Y.C., D.S., Y.L., and Y.S.; Formal analysis, D.S.; Investigation, W.Z.; Resources, Y.C. and N.Z.;Data curation, Y.C. and D.S.; Writing—original draft preparation, D.S.; Writing—review and editing, Y.C. and Y.S.;Visualization, D.S.; Supervision, D.S.; Project administration, Y.L.; Funding acquisition. All authors have read and agreed to the published version of the manuscript.

Funding: The research was supported by the China Postdoctoral Science Foundation (Grant No. 2023M733468) and General Program of National Natural Science Foundation of China (Grant No. 41271186).

Data Availability Statement

Acknowledgments

Conflicts of Interest: The authors declare no conflict of interest.

References

1. Ampatzidis, P.; Kershaw, T. A review of the impact of blue space on the urban microclimate. *Sci. Total Environ.* **2020**, *730*, 139068; DOI:10.1016/j.scitotenv.2020.139068.
2. Foley, J.A.; Defries, R.; Asner, G.P.; Barford, C.; Bonan, G.; Carpenter, S.R.; Chapin, F.S.; Coe, M.T.; Daily, G.C.; Gibbs, H.K.; et al. Global consequences of land use. *Science* **2005**, *309*, 570–574; DOI:10.1126/science.1111772.
3. Gunawardena, K.R.; Wells, M.J.; Kershaw, T. Utilising green and bluespace to mitigate urban heat Island intensity. *Sci. Total Environ.* **2017**, *584-585*, 1040–1055; DOI:10.1016/j.scitotenv.2017.01.158.
4. Perosa, F.; Fanger, S.; Zingraff-Hamed, A.; Disse, M. A meta-analysis of the value of ecosystem services of floodplains for the Danube River Basin. *Sci. Total Environ.* **2021**, *777*, 146062; DOI:10.1016/j.scitotenv.2021.146062.
5. Georgiou, M.; Tieges, Z.; Morison, G.; Smith, N.; Chastin, S. A population-based retrospective study of the modifying effect of urban blue space on the impact of socioeconomic deprivation on mental health, 2009-2018. *Sci. Rep.* **2022**, *12*, 13040; DOI:10.1038/s41598-022-17089-z.
6. Martínez-Arroyo, A.; Jáuregui, E. On the environmental role of urban lakes in Mexico city. *Urban Ecosyst.* **2000**, *4*, 145–166; DOI:10.1023/A:1011355110475.
7. He, B.J.; Zhu, J.; Zhao, D.; Gou, Z.H.; Qi, J.D.; Wang, J. Co-benefits approach: Opportunities for implementing sponge city and urban heat island mitigation. *Land Use Policy* **2019**, *86*, 147–157; DOI:10.1016/j.landusepol.2019.05.003.
8. Adams, K.D.; Sada, D.W. Surface water hydrology and geomorphic characterization of a playa lake system: Implications for monitoring the effects of climate change. *J. Hydrol.* **2014**, *510*, 92–102; DOI:10.1016/j.jhydrol.2013.12.018.
9. Joosse, S.; Hensle, L.; Boonstra, W.J.; Ponzelar, C.; Olsson, J. Fishing in the city for food—A paradigmatic case of sustainability in urban blue space. *NPJ Urban Sustain.* **2021**, *1*, 41; DOI:10.1038/s42949-021-00043-9.
10. Anderson, E.P.; Jackson, S.; Tharme, R.E.; Douglas, M.; Flotemersch, J.E.; Zwarteveen, M.; Lokgariwar, C.; Montoya, M.; Wali, A.; Tipa, G.T.; et al. Understanding rivers and their social relations: A critical step to advance environmental water management. *WIREs Water* **2019**, *6*, e1381; DOI:10.1002/wat2.1381.
11. Chang, N.; Luo, L.; Wang, X.C.; Song, J.; Han, J.; Ao, D. A novel index for assessing the water quality of urban landscape lakes based on water transparency. *Sci. Total Environ.* **2020**, *735*, 139351; DOI:10.1016/j.scitotenv.2020.139351.
12. Yu, H.; Song, Y.; Chang, X.; Gao, H.; Peng, J. A scheme for a sustainable urban water environmental system during the urbanization process in China. *Engineering* **2018**, *4*, 190–193; DOI:10.1016/j.eng.2018.03.009.
13. Coutts, A.M.; Tapper, N.J.; Beringer, J.; Loughnan, M.; Demuzere, M. Watering our cities: The capacity for water sensitive urban design to support urban cooling and improve human thermal comfort in the Australian context. *Prog. Phys. Geogr. Earth Environ.* **2013**, *37*, 2–28; DOI:10.1177/0309133312461032.
14. Völker, S.; Kistemann, T. Developing the urban blue: Comparative health responses to blue and green urban open spaces in Germany. *Health Place* **2015**, *35*, 196–205; DOI:10.1016/j.healthplace.2014.10.015.
15. Wang, M.; Du, L.; Ke, Y.; Huang, M.; Zhang, J.; Zhao, Y.; Li, X.; Gong, H. Impact of climate variabilities and human activities on surface water extents in reservoirs of Yongding River Basin, China, from 1985 to 2016 based on landsat observations and time series analysis. *Remote Sens.* **2019**, *11*, 560; DOI:10.3390/rs11050560.
16. Liu, L.; Fryd, O.; Zhang, S. Blue-green infrastructure for sustainable urban stormwater management—Lessons from six municipality-led pilot projects in Beijing and Copenhagen. *Water* **2019**, *11*, 2024; DOI:10.3390/w11102024.
17. Huang, H.; Yang, H.; Chen, Y.; Chen, T.; Bai, L.; Peng, Z.R. Urban green space optimization based on a climate health risk appraisal – A case study of Beijing city, China. *Urban For. Urban Green.* **2021**, *62*, 127154; DOI:10.1016/j.ufug.2021.127154.
18. Helbich, M.; Yao, Y.; Liu, Y.; Zhang, J.; Liu, P.; Wang, R. Using deep learning to examine street view green and blue spaces and their associations with geriatric depression in Beijing, China. *Environ. Int.* **2019**, *126*, 107–117; DOI:10.1016/j.envint.2019.02.013.
19. Dou, Y.; Zhen, L.; De Groot, R.; Du, B.; Yu, X. Assessing the importance of cultural ecosystem services in urban areas of Beijing municipality. *Ecosyst. Serv.* **2017**, *24*, 79–90; DOI:10.1016/j.ecoser.2017.02.011.
20. Gašparović, S.; Sopina, A.; Zeneral, A. Impacts of Zagreb's urban development on dynamic changes in stream landscapes from mid-twentieth century. *Land* **2022**, *11*, 692; DOI:10.3390/land11050692.

21. Hysa, A. Introducing transversal connectivity index (TCI) as a method to evaluate the effectiveness of the blue-green infrastructure at metropolitan scale. *Ecol. Indic.* **2021**, *124*, 107432; DOI:10.1016/j.ecolind.2021.107432.
22. Luo, S.; Xie, J.; Furuya, K. Assessing the preference and restorative potential of urban park blue space. *Land* **2021**, *10*, 1233; DOI:10.3390/land10111233.
23. Zhao, J.; Guo, W.; Huang, W.; Huang, L.; Zhang, D.; Yang, H.; Yuan, L. Characterizing spatiotemporal dynamics of land cover with multi-temporal remotely sensed imagery in Beijing during 1978–2010. *Arab. J. Geosci.* **2014**, *7*, 3945–3959; DOI:10.1007/s12517-013-1072-5.
24. Wu, J.; Yang, S.; Zhang, X. Interaction analysis of urban blue-green space and built-up area based on coupling model—A case study of Wuhan central city. *Water* **2020**, *12*, 2185; DOI:10.3390/w12082185.
25. Wang, S.; Yang, K.; Yuan, D.; Yu, K.; Su, Y. Temporal-spatial changes about the landscape pattern of water system and their relationship with food and energy in a mega city in China. *Ecol. Model.* **2019**, *401*, 75–84; DOI:10.1016/j.ecolmodel.2019.02.010.
26. Cao, H.; Liu, J.; Chen, J.; Gao, J.; Wang, G.; Zhang, W. Spatiotemporal patterns of urban land use change in typical cities in the greater mekong subregion (GMS). *Remote Sens.* **2019**, *11*, 801; DOI:10.3390/rs11070801.
27. Xie, Y.; Wang, G.; Wang, X.; Fan, P. Assessing the evolution of oases in arid regions by reconstructing their historic spatio-temporal distribution: A case study of the Heihe River Basin, China. *Front. Earth Sci.* **2017**, *11*, 629–642; DOI:10.1007/s11707-016-0607-y.
28. Song, S.; Wang, S.; Shi, M.; Hu, S.; Xu, D. Urban blue–green space landscape ecological health assessment based on the integration of pattern, process, function and sustainability. *Sci. Rep.* **2022**, *12*, 7707; DOI:10.1038/s41598-022-11960-9.
29. Liu, Y.; Zhang, D.; He, K.; Gao, Q.; Qin, F. Research on land use change and ecological environment effect based on remote sensing sensor technology. *J. Sens.* **2021**, *2021*, 4351733; DOI:10.1155/2021/4351733.
30. Hurford, A.P.; Parker, D.J.; Priest, S.J.; Lumbroso, D.M. Validating the return period of rainfall thresholds used for extreme rainfall alerts by linking rainfall intensities with observed surface water flood events. *J. Flood Risk Manag.* **2012**, *5*, 134–142; DOI:10.1111/j.1753-318X.2012.01133.x.
31. Brinkmann, K.; Hoffmann, E.; Buerkert, A. Spatial and temporal dynamics of urban wetlands in an Indian megacity over the past 50 years. *Remote Sens.* **2020**, *12*, 662; DOI:10.3390/rs12040662.
32. Suligowski, R.; Ciupa, T.; Cudny, W. Quantity assessment of urban green, blue, and grey spaces in Poland. *Urban For. Urban Green.* **2021**, *64*, 127276; DOI:10.1016/j.ufug.2021.127276.
33. Steele, M.K.; Heffernan, J.B. Morphological characteristics of urban water bodies: Mechanisms of change and implications for ecosystem function. *Ecol. Appl.* **2014**, *24*, 1070–1084; DOI:10.1890/13-0983.1.
34. Elmore, A.J.; Kaushal, S.S. Disappearing headwaters: Patterns of stream burial due to urbanization. *Front. Ecol. Environ.* **2008**, *6*, 308–312; DOI:10.1890/070101.
35. Brans, K.I.; Engelen, J.M.T.; Souffreau, C.; De Meester, L. Urban hot-tubs: Local urbanization has profound effects on average and extreme temperatures in ponds. *Landsc. Urban Plan.* **2018**, *176*, 22–29; DOI:10.1016/j.landurbplan.2018.03.013.
36. Peng, J.; Liu, Q.; Xu, Z.; Lyu, D.; Du, Y.; Qiao, R.; Wu, J. How to effectively mitigate urban heat island effect? A perspective of waterbody patch size threshold. *Landsc. Urban Plan.* **2020**, *202*, 103873; DOI:10.1016/j.landurbplan.2020.103873.
37. Holder, C.D.; Gibbes, C. Influence of leaf and canopy characteristics on rainfall interception and urban hydrology. *Hydrol. Sci. J.* **2017**, *62*, 182–190; DOI:10.1080/02626667.2016.1217414.
38. Walsh, C.J.; Roy, A.H.; Feminella, J.W.; Cottingham, P.D.; Groffman, P.M.; Morgan, R.P. The urban stream syndrome: Current knowledge and the search for a cure. *J. N. Am. Benthol. Soc.* **2005**, *24*, 706–723; DOI:10.1899/04-028.1.
39. Pan, H.; Deal, B.; Destouni, G.; Zhang, Y.; Kalantari, Z. Sociohydrology modeling for complex urban environments in support of integrated land and water resource management practices. *Land Degrad. Dev.* **2018**, *29*, 3639–3652; DOI:10.1002/ldr.3106.
40. Clare, S.; Krogman, N.; Foote, L.; Lemphers, N. Where is the avoidance in the implementation of wetland law and policy? *Wetl. Ecol. Manag.* **2011**, *19*, 165–182; DOI:10.1007/s11273-011-9209-3.
41. Leigh, N.G.; Lee, H. Sustainable and resilient urban water systems: The role of decentralization and planning. *Sustainability* **2019**, *11*, 918; DOI:10.3390/su11030918.
42. Ianoş, I.; Sorensen, A.; Merciu, C. Incoherence of urban planning policy in Bucharest: Its potential for land use conflict. *Land Use Policy* **2017**, *60*, 101–112; DOI:10.1016/j.landusepol.2016.10.030.
43. Jiang, T.T.; Pan, J.F.; Pu, X.M.; Wang, B.; Pan, J.J. Current status of coastal wetlands in China: Degradation, restoration, and future management. *Estuar. Coast. Shelf Sci.* **2015**, *164*, 265–275; DOI:10.1016/j.ecss.2015.07.046.
44. Völker, S.; Kistemann, T. The impact of blue space on human health and well-being – Salutogenetic health effects of inland surface waters: A review. *Int. J. Hyg. Environ. Health* **2011**, *214*, 449–460; DOI:10.1016/j.ijheh.2011.05.001.

45. Pandey, C.L. Managing urban water security: Challenges and prospects in Nepal. *Environ. Dev. Sustain.* **2021**, *23*, 241–257; DOI:10.1007/s10668-019-00577-0.
46. Zhong, Q.; Ma, J.; Zhao, B.; Wang, X.; Zong, J.; Xiao, X. Assessing spatial-temporal dynamics of urban expansion, vegetation greenness and photosynthesis in megacity Shanghai, China during 2000–2016. *Remote Sens. Environ.* **2019**, *233*, 111374; DOI:10.1016/j.rse.2019.111374.
47. Karmaoui, A.; Ben Salem, A.; El Jaafari, S.; Chaachouay, H.; Moumane, A.; Hajji, L. Exploring the land use and land cover change in the period 2005–2020 in the province of Errachidia, the pre-sahara of Morocco. *Front. Earth Sci.* **2022**, *10*, 962097; DOI:10.3389/feart.2022.962097.
48. Investing general situation of Beijing. Available online: http://www.beijing.gov.cn/renwen/bjgk/ (accessed on 4 April 2023).
49. The People's Government of Beijing Municipality. Beijing 2021 statistical bulletin on national economic and social development. Available online: https://www.beijing.gov.cn/gongkai/shuju/tjgb/202203/t20220301_2618806.html (accessed on 1 March 2022).
50. Peel, M.C.; Finlayson, B.L.; McMahon, T.A. Updated world map of the Köppen-Geiger climate classification. *Hydrol. Earth Syst. Sci.* **2007**, *11*, 1633–1644; DOI:10.5194/hess-11-1633-2007.
51. Congalton, R.G. A review of assessing the accuracy of classifications of remotely sensed data. *Remote Sens. Environ.* **1991**, *37*, 35–46; DOI:10.1016/0034-4257(91)90048-B.
52. Anselin, L. Local indicators of spatial association—LISA. *Geogr. Anal.* **1995**, *27*, 93–115; DOI:10.1111/j.1538-4632.1995.tb00338.x.
53. Moran, P.A.P. The interpretation of statistical maps. *J. R. Stat. Soc. B (Methodol.)* **1948**, *10*, 243–251; DOI:10.1111/j.2517-6161.1948.tb00012.x.
54. Cheng, X.; Wallace, J.M. Cluster analysis of the northern hemisphere wintertime 500-hPa height field: Spatial patterns. *J. Atmos. Sci.* **1993**, *50*, 2674–2696; DOI:10.1175/1520-0469(1993)050<2674:CAOTNH>2.0.CO;2.
55. ArcGIS Resource. ArcGIS resource center. Available online: http://resources.arcgis.com/zh-cn/help/main/10.2/ (accessed on 5 May 2023).
56. Chang, C.W.; Laird, D.A.; Mausbach, M.J.; Hurburgh, C.R. Near-infrared reflectance spectroscopy–principal components regression analyses of soil properties. *Soil Sci. Soc. Am. J.* **2001**, *65*, 480–490; DOI:10.2136/sssaj2001.652480x.
57. Wentzell, P.D.; Montoto, L.V. Comparison of principal components regression and partial least squares regression through generic simulations of complex mixtures. *Chemom. Intell. Lab. Syst.* **2003**, *65*, 257–279; DOI:10.1016/S0169-7439(02)00138-7.
58. Deng, J.L. Control problems of grey systems. *Syst. Control Lett.* **1982**, *1*, 288–294; DOI:10.1016/S0167-6911(82)80025-X.
59. Liu, S.F.; Xie, N.M.; Forrest, J. On new models of grey incidence analysis based on visual angle of similarity and nearness. *Syst. Eng. Theory Pract.* **2010**, *30*, 881–887; DOI:10.1000-6788(2010)05-0881-07.
60. Sun, F. Discussion on grey correlation analysis method and its application. *Sci. Technol. Inf.* **2010**, *17*, 880–882; DOI:10.1016/j.jamcollsurg.2010.02.031.
61. Raymond, C.M.; Gottwald, S.; Kuoppa, J.; Kyttä, M. Integrating multiple elements of environmental justice into urban blue space planning using public participation geographic information systems. *Landsc. Urban Plan.* **2016**, *153*, 198–208; DOI:10.1016/j.landurbplan.2016.05.005.
62. Bedla, D.; Halecki, W. The value of river valleys for restoring landscape features and the continuity of urban ecosystem functions – A review. *Ecol. Indic.* **2021**, *129*, 107871; DOI:10.1016/j.ecolind.2021.107871.
63. Avashia, V.; Garg, A. Implications of land use transitions and climate change on local flooding in urban areas: An assessment of 42 Indian cities. *Land Use Policy* **2020**, *95*, 104571; DOI:10.1016/j.landusepol.2020.104571.
64. Dai, X.; Wang, L.; Tao, M.; Huang, C.; Sun, J.; Wang, S. Assessing the ecological balance between supply and demand of blue-green infrastructure. *J. Environ. Manag.* **2021**, *288*, 112454; DOI:10.1016/j.jenvman.2021.112454.
65. Yu, Z.; Yang, G.; Zuo, S.; Jørgensen, G.; Koga, M.; Vejre, H. Critical review on the cooling effect of urban blue-green space: A threshold-size perspective. *Urban For. Urban Green.* **2020**, *49*, 126630; DOI:10.1016/j.ufug.2020.126630.
66. Taramelli, A.; Lissoni, M.; Piedelobo, L.; Schiavon, E.; Valentini, E.; Nguyen Xuan, A.; González-Aguilera, D. Monitoring green infrastructure for natural water retention using Copernicus global land products. *Remote Sens.* **2019**, *11*, 1583; DOI:10.3390/rs11131583.
67. Crisigiovanni, E.; Nascimento, E.; Godoy, R.; Filho, P.; Vidal, C.; Martins, K.G. Inadequate riparian zone use directly decreases water quality of a low-order urban stream in southern Brazil. *Rev. Ambiente Água* **2020**, *15*, e2451; DOI:10.4136/ambi-agua.2451.
68. Carraça, M.G.D.; Collier, C.G. Modelling the impact of high-rise buildings in urban areas on precipitation initiation. *Meteorol. Appl.* **2007**, *14*, 149–161; DOI:10.1002/met.15.

69. Yang, G.; Yu, Z.; Jørgensen, G.; Vejre, H. How can urban blue-green space be planned for climate adaption in high-latitude cities? A seasonal perspective. *Sustain. Cities Soc.* **2020**, *53*, 101932; DOI:10.1016/j.scs.2019.101932.
70. Li, X.; Stringer, L.C.; Dallimer, M. The role of blue green infrastructure in the urban thermal environment across seasons and local climate zones in East Africa. *Sustain. Cities Soc.* **2022**, *80*, 103798; DOI:10.1016/j.scs.2022.103798.
71. Zhang, H.; Wang, X.; Ho, H.H.; Yong, Y. Eco-health evaluation for the Shanghai metropolitan area during the recent industrial transformation (1990–2003). *J. Environ. Manag.* **2008**, *88*, 1047–1055; DOI:10.1016/j.jenvman.2007.05.008.
72. Shifaw, E.; Sha, J.; Li, X.; Jiali, S.; Bao, Z. Remote sensing and GIS-based analysis of urban dynamics and modelling of its drivers, the case of Pingtan, China. *Environ. Dev. Sustain.* **2020**, *22*, 2159–2186; DOI:10.1007/s10668-018-0283-z.
73. Das, A.; Basu, T. Assessment of peri-urban wetland ecological degradation through importance-performance analysis (IPA): A study on Chatra Wetland, India. *Ecol. Indic.* **2020**, *114*, 106274; DOI:10.1016/j.ecolind.2020.106274.
74. Sun, Y.; Shen, L.; Lu, C. Study on the water footprint and external water dependency of Beijing. *Water Supply* **2016**, *16*, 1077–1085; DOI:10.2166/ws.2016.022.
75. Liu, J.; Wang, D.; Xiang, C.; Xia, L.; Zhang, K.; Shao, W.; Luan, Q. Assessment of the energy use for water supply in Beijing. *Energy Procedia* **2018**, *152*, 271–280; DOI:10.1016/j.egypro.2018.09.122.
76. China Weather Network. Weather and climate characteristics in Beijing during flood season in 2015. Available online: http://bj.weather.com.cn/sygdt/09/2391386.shtml (accessed on 4 April 2023).
77. Zhou, C.; Lan, H.; Gong, H.; Zhang, Y.; Warner, T.A.; Clague, J.J.; Wu, Y. Reduced rate of land subsidence since 2016 in Beijing, China: Evidence from Tomo-PSInSAR using RadarSAT-2 and Sentinel-1 datasets. *Int. J. Remote Sens.* **2020**, *41*, 1259–1285; DOI:10.1080/01431161.2019.1662967.
78. The People's Government of Beijing Municipality. Policies on the prevention and control of water pollution in Beijing. Available online: http://www.beijing.gov.cn/zhengce/zhengcefagui/201905/t20190522_58901.html (accessed on 4 April 2023).
79. Sun, R.; Chen, L. How can urban water bodies be designed for climate adaptation? *Landsc. Urban Plan.* **2012**, *105*, 27–33; DOI:10.1016/j.landurbplan.2011.11.018.
80. The People's Government of Beijing Municipality. Beijing further accelerated the implementation of the three-year action plan for sewage treatment and reclaimed water utilization. Available online: http://www.beijing.gov.cn/zhengce/zhengcefagui/201907/t20190701_100007.html (accessed on 4 April 2023).
81. Tu, W.; Hu, Z.; Li, L.; Cao, J.; Jiang, J.; Li, Q.; Li, Q. Portraying urban functional zones by coupling remote sensing imagery and human sensing data. *Remote Sens.* **2018**, *10*, 141; DOI:10.3390/rs10010141.
82. Blue and green interwoven, water and city in harmony -- A brief account of ecological environment construction of Beijing city sub-center. Available online: https://baijiahao.baidu.com/s?id=1725324278643150074&wfr=spider&for=pc (accessed on 4 April 2023).